The ability of three African herbal remedies to offer protection against an *in vitro* model of Parkinson's disease

Keagile H Lepule,[1] Werner Cordier,[1]Paul Steenkamp,[2] Margo Nell,[1] Vanessa Steenkamp[1*]

[1]*Department of Pharmacology, Faculty of Health Sciences, University of Pretoria, Pretoria, South Africa*

[2]*Centre for Plant Metabolomics Research, Department of Biochemistry, University of Johannesburg, Auckland Park, South Africa*

***Corresponding author details:**

Corresponding author: Prof Vanessa Steenkamp

Postal address: Department of Pharmacology, Faculty of Health Sciences, School of Medicine, University of Pretoria, Private Bag X323, Arcadia, 0007, Pretoria, South Africa

Contact number: +27 12 319 2547

E-mail address: vanessa.steenkamp@up.ac.za

Highlights

- Acetone and methanol extracts of *X. undulatum* reduced 6-OHDA-induced cytotoxicity.
- Concentrations as low as 0.5 µg/mL reduced cytotoxicity.
- Mitochondrial integrity was not improved, but oxidative stress was decreased.
- Cytoprotection was observed in morphological assessment.

Abbreviations: 6-OHDA: 6-hydroxydopamine, ATP: adenosine tri-phosphate, Ca^{2+}: calcium, ETC: electron transport chain, GSH: reduced glutathione, HDMS: high definition mass spectrometry IC_{50}: half maximal inhibitory concentrations, JC-1: 5,5,'6,6'-Tetrachloro-1,1,3,3'- tetraethylbenzimidazolylcarbocyanine iodide, MCB: monochlorobimane, MMP: mitochondrial membrane potential, ROS: reactive oxygen species, PDA: photodiode array, PlasDIC: polarisation-optical transmitted light differential interference contrast microscopy, PD: Parkinson's disease, SRB: sulforhodamine B, UPLC: ultra-performance liquid chromatography.

Abstract

Parkinson's disease, characterised by loss of dopaminergic neurons in the substantia nigra of the brain, is attributed to oxidative stress and mitochondrial dysfunction. As no cure is available, and dopamine-replacement therapy only offers symptomatic relief, other avenues of treatment are sought. *Acokanthera oppositifolia*, *Boophone disticha* and *Xysmalobium undulatum* are used ethnomedicinally for the treatment of neurological disorders, however, these plants have not been assessed *in vitro* for cytoprotective activity. The aim of the study was to assess the cytoprotective activity of these three plants in an *in vitro* SH-SY5Y cellular model of Parkinson's disease induced by 6-hydroxydopamine (6-OHDA).

Plant material was extracted using acetone and methanol ultrasonic maceration. Cytotoxicity was induced by exposing cells to 33.3 µM 6-OHDA for 2 h, followed by 24 h incubation with the crude extracts. Ultra-performance liquid chromatography high definition mass spectrometry was used for tentative identification of phytochemicals. Cytoprotection was initially assessed using the sulforhodamine B staining assay to determine concentration ranges. Mitochondrial membrane potential (MMP), reactive oxygen species (ROS) levels, reduced glutathione (GSH) content, intracellular Ca^{2+} flux and ATP levels were assessed using the JC-1 ratiometric, dihydrodichlorofluorescein cleavage, monochlorobamine adduct formation, Fura-2AM and bioluminescence assays, respectively. Cell morphology was visualized using polarisation-optical transmitted light differential interference contrast microscopy.

Several phytochemicals were tentatively identified that are known markers in the plant species, however, little difference was noted between the acetone and methanol extracts qualitatively. Neurotoxicity reduced cell density by 91%, increased ROS (217.7%) and GSH (102.1%) levels. Mitochondrial depolarisation (54.2%) was evident. Crude extracts attenuated cytotoxicity by reducing ROS and sustaining ATP production, however, no alteration to MMP was observed. Furthermore, Ca^{2+} effects were maintained by *B. disticha* and *X. undulatum*, but reduced by *A. oppositifolia*. Morphological changes characteristic of cytotoxicity was observed when exposed to 6-OHDA was observed in micrographs. Intermediate-polarity extracts reduced the detrimental effects associated with 6-OHDA-induced cytotoxicity. *X. undulatum* (5 µg/mL) displayed the greatest level of cytoprotection, however, the inherent cytotoxicity may limit the usefulness of extracts during treatment of disease.

Although none of the plant extracts showed potential to reverse *in vitro* characteristics of Parkinson's disease completely, concomitant use with dopamine replacement therapy should be investigated as a possible treatment modality. Adjunct use of the crude extracts with traditional dopamine replacement therapy may offer an alternative approach, however, future studies are required to elucidate the feasibility of such a combination.

Keywords: *Acokanthera oppositifolia*, *Boophone disticha,* Parkinson's disease, plant extracts, preventative treatment, *Xysmalobium undulatum*.

1. Introduction

Parkinson's disease (PD) is the second most common neurodegenerative disease, affecting 1% of those >60 years of age, with a lifetime risk of ~1.5% (Kim *et al*., 2006; Lees *et al*., 2009). The world prevalence is estimated to double by 2030 (Kakkar and Dahiya, 2015). Parkinson's disease is characterised by irreversible dopaminergic neuron loss in the pars compacta of the substantia nigra of the brain (Banerjee *et al*., 2009), with subsequent hypodopaminergic activity (Kim *et al*., 2006; Banerjee *et al*., 2009; Ham *et al*., 2012). Mitochondrial dysfunction with oxidative stress is implicated in the neuron loss (Kim *et al*., 2006). As no cure exists for PD, treatment remains symptomatic, primarily focusing on dopamine replacement (Lees *et al*., 2009; Kakkar and Dahiya, 2015; Yadav and Li, 2015). Treatment becomes inefficient with disease progression due to continuous neuronal loss. It has been suggested that neuroprotective measures are needed to delay worsening of the disease as it progresses (Stayte and Vissel, 2014).

Mitochondrial dysfunction has been implicated as an underlying cause of PD. The mitochondrion plays a key role in the coordination of mitochondrial-dependent apoptosis via the mitochondrial permeability transition pore (Ly *et al*., 2003). Mitochondrial membrane depolarisation opens the mitochondrial permeability transition pore. When excessive opening occurs, pro-death mediators are released, subsequently inducing cell death pathways (Ly *et al*., 2003). Furthermore, mitochondrial membrane potential (MMP) needs to be maintained for bioenergetic functioning to occur, such as generation of adenosine tri-phosphate (ATP) (Ly *et al*., 2003). Mitochondrial dysfunction produces reactive oxygen species (ROS), which aggravates PD (Reddy and Reddy, 2011). Reactive oxygen species are produced as metabolic by-products to function as signalling molecules, which in excess may cause oxidative stress with subsequent damage to macromolecules and cell death (Reddy and Reddy, 2011). Such high levels of ROS decreases intracellular antioxidant stores, including reduced glutathione (GSH), promoting cytotoxicity. The latter has been linked to PD (Ruszkiewicz and Albrecht, 2015): buthionine sulfoximine (an inhibitor of GSH synthesis) induces PD-like characteristics both *in vitro* and *in vivo*, giving credence to the GSH-deficiency hypothesis (Bharath *et al*., 2002). Reduced glutathione depletion may incur oxidative stress (Bhat *et al*., 2015) and ultimately induce electron transport chain (ETC) dysfunction (McBean *et al*. 2015).

Adenosine tri-phosphate is an energy-rich molecule that is required for maintaining physiological processes. Production thereof is dependent on glycolysis, the Krebs cycle and the ETC (Cairns *et al*., 2011). Oxidative phosphorylation on the other hand is an oxygen-dependent pathway that couples oxidation of macromolecules to the ETC to generate ATP (Cairns *et al*., 2011). In PD models, the oxidative pathway is hindered by blocking mitochondrial complex I, thus impairing ATP production, generating ROS, and subsequently inducing cell death (Cabezas *et al*., 2013). Calcium is one of the most regulated ions in the cell. Homeostasis of intracellular Ca^{2+} requires high amounts of energy, as cells prefer to store Ca^{2+} in endoplasmic reticulum and mitochondria, which is released after appropriate stimulation (Contreras *et al*., 2010; Abeti and Abramov, 2015). Mitochondrial-stored Ca^{2+}, together with H^{+}, drives ATP production (Abeti and Abramov, 2015). However, in PD the production of ATP is hindered, hence a subsequent intracellular Ca^{2+} overload is observed (Abeti and Abramov, 2015).

6-Hydroxydopamine (6-OHDA) is a recognised neurotoxin used for studying PD-like effects *in vitro* by interfering with the ETC and cellular redox capacity by blocking mitochondrial complex I (Mazzio *et al*., 2004; Lopes *et al*., 2010). This subsequently depolarises the mitochondrial membrane, diminishes ATP production and promotes ROS formation (Blum *et al*., 2001; Mazzio *et al*., 2004; Lopes *et al*., 2010). Mitochondrial defects induced by 6-OHDA stimulate the opening of the mitochondrial permeability transition pore which releases pro-apoptotic factors to induce apoptosis (Blum *et al*., 2001; Mazzio *et al*., 2004).

There is a dire need to discover drugs which could attenuate the aforementioned processes. Various herbal remedies have been shown to offer neuroprotection, thus it may serve as a viable platform for drug discovery. *Acokanthera oppositifolia* (Lam.) Codd (Apocynaceae) is known by locals as the 'common poison bush' (English), 'gewone gifboom' (Afrikaans) and 'uhlunguyembe' (Zulu) (van Wyk *et al*., 2009). *A. oppositifolia* is traditionally used for treating headaches and convulsions (Adedapo *et al*., 2008; van Wyk *et al*., 2009; Sharma and Chaurasia, 2014). *Boophone disticha* (L.f.) Herb (Amaryllidaceae) is commonly known as 'bushman poison bulb' (English), 'gifbol' (Afrikaans) and 'incotha' (Zulu) (van Wyk *et al*., 2009). The bulb of *B. disticha* is used to treat paralysis, age-related dementia and headaches, and is known to induce hallucinations (van Wyk *et al*., 2009; Nair and van Staden, 2014). *Xysmalobium undulatum* (L.) Aiton.F. (Apocynaceae) is marketed as uzara. The roots of *X. undulatum* are used to treat hysteria and headaches, as well as for sedation (Stafford *et al*., 2008; van Wyk *et al*., 2009). The aim of this study was to evaluate the cytoprotective effects of the aforementioned three African medicinal plants using 6-OHDA-induced neurotoxicity in the SH-SY5Y human neuroblastoma cell line as model of PD.

2. Materials and methods

2.1. Reagents

Acetone and methanol were obtained from Merck Chemicals (Darmstadt, Germany), while BBL™ FTA haemagluttination buffer (used for phosphate-buffered saline preparation) was obtained from BD Biosciences (France). All other reagents were obtained from Sigma-Aldrich (St. Louis, USA).

2.2. Extraction of plant material

Plant material was dried, ground and stored in amber bottles until needed. *A. oppositifolia* (roots) was collected in the wild by Mr Lawrence Tshikudo, and a voucher specimen deposited at the Department of Toxicology (LT0019; Onderstepoort Veterinary Institute, Pretoria). *B. disticha* (bulb) and *X. undulatum* (roots) were received as gifts from the South African Natural Biodiversity Institute (SANBI, Pretoria) after confirmation by their in-house botanist.

Crude extracts were prepared for drug discovery purposes using intermediate polarity solvents that have a higher likelihood of achieving blood-brain barrier permeability. Acetone and methanol extracts were prepared by sonicating 10 g sample in 100 mL respective solvent for 30 min. The mixture was agitated for 30 min and macerated overnight at 4˚C. The supernatant was collected through centrifugation at 1 000 *g* for 5

min, and the pelleted plant material re-extracted overnight with the same solvent. All respective collected supernatants were combined. Extracts were syringe-filtered (0.22 µm), and the filtrate concentrated using vacuum rotary evaporation (Büchi Rotovapor R-200, Büchi). Dried extracts were re-dissolved in dimethyl sulfoxide (DMSO) and stored at -80 °C to prevent phytochemical decomposition. Yields were determined gravimetrically.

2.3. Phytochemical profiling

Chemical profiling of phytochemicals was performed using ultra-performance liquid chromatography (UPLC; Waters) coupled in tandem to a photodiode array (PDA; Waters) detector and high-definition mass spectrometer (HDMS; SYNAPT G1, Waters). A Waters HSS T3 C18 column (150 mm × 2.1 mm, 1.8 µm; 60ºC) was used to optimise separation with ultrapure LC-MS grade solvents. Crude extracts were re-dissolved in methanol to 10 mg/mL and filtered (0.2 µm) prior to analysis. The solvent mixture consisted of 10 mM aqueous formic acid (pH 2.3) (solvent A) and 10 mM formic acid in acetonitrile (solvent B). The run (0.4 mL/min flow rate; 20 min; 3 µL; triplicate injections) was initiated at 100% solvent A mobile phase for 1 min, followed by a linear gradient to 5% solvent A mobile phase at 16 min, which was maintained for 1 min prior to reverting to the initial conditions. Detection using the PDA occurred between 200 and 500 nm (1.2 nm resolution), collecting 20 spectra per second.

The SYNAPT G1 HDMS was used in V-optics and operated in electrospray mode to allow for phenolic and other electro spray ionization (ESI)-compatible compound detection. Reference calibration was done using leucine enkephalin (50 pg/mL) to obtain typical mass accuracies between 1 and 5 mDa. The mass spectrometer was operated in both negative and positive mode. Capillary voltage, sampling cone and extraction cone parameters were set at 2.5 kV, 30 V and 4.5 V, respectively. The scan time was 0.1 s covering a 50 to 1 200 Da mass range. Source and desolvation temperature were set at 120 °C and 450 °C, respectively. Nebulisation gas (nitrogen gas) was set at a flow rate of 550 L/h, and cone gas added at 50 L/h. Analysis was done using MassLynx 4.1 (SCN 872) software.

2.4. Cell culture and maintenance

The SH-SY5Y neuroblastoma cell line (ATCC CRL-2266) was a gift from the Department of Pharmacology, North-West University. Cells were cultured in a 1:1 mixture of Ham's F12 medium and Dulbecco's Modified Eagle's Medium (DMEM) supplemented with 1% non-essential amino acids, 1% L-glutamine, penicillin (100 U/mL), streptomycin (100 U/mL) and 10% heat-inactivated foetal calf serum (FCS) at 37^{o}C in a humidified incubator with a 5% CO_2 atmosphere. Confluent cells (80%) were washed with sterilised phosphate-buffered saline (PBS) and chemically detached with Trypsin/Versene solution. Cells were harvested at 200 *g* for 5 min and the pellet re-suspended in 1 mL medium. Cells were counted using the trypan blue exclusion assay (0.1% w/v) and re-suspended to 2.5 x 10^5 cells/mL or 1 x 10^5 cells/mL for the 24-well and 96-well plate assays.

2.5. Cytotoxicity of crude extracts on cell density

The sulforhodamine B (SRB) assay was conducted according to Vichai and Kirtikara (Vichai and Kirtikara, 2006) with minor modifications to volumes. Seeded cells (100 µL) were incubated in 96-well plates overnight to allow for attachment. Cells were exposed to 100 µL medium (negative control), acidified control (pH 5.8), 0.5% DMSO (vehicle control), 1% saponin (positive control), or crude extracts (2 - 200 µg/mL) prepared in FCS-free medium for 48 h. Blanks consisted of 5% FCS-supplemented medium alone to account for sterility and background noise. After incubation, cells were fixed with 50 µL trichloroacetic acid (50% v/v) overnight at 4°C. After fixation, plates were washed twice with tap water, dried and stained with 100 µL SRB solution (0.057% w/v in 1% v/v acetic acid) for 30 min. Excess dye was removed by rinsing plates thrice with 1% acetic acid. Bound dye was dissolved using 200 µL Tris-base solution (10 mM, pH 10.5) for 30 min on a shaker. Plates were read spectrophotometrically using an EL-X 800 microplate reader (Biotek Inc, USA) at 510 nm (reference wavelength of 630 nm). Values were blank-excluded and cell density determined by the following equation:

$$\text{Cell density (\% of negative control)} = \left(\frac{\text{absorbance of sample}}{\text{average absorbance of negative control}}\right) \times 100$$

2.6. Cytoprotective effects of crude extracts in the Parkinson's disease model

6-Hydroxydopamine was used to establish PD-like effects in the neurotoxicity model with a concentration optimised in-house to induce moderate reductions in cell density (IC_{50} = 23.4 µM; data not shown). The working solutions of 6-OHDA were prepared in acetic acid-acidified medium (pH 5.8) to promote solubility. To assess the cytoprotection offered by the crude extracts, cells were seeded as described in Section 2.4 and exposed to 6-OHDA (50 µL, 33.3 µM) for 2 h. Cells were treated with 50 µL crude extracts at 2, 4, 20, 60 and 120 µg/mL (0.5, 1, 5, 15 and 30 µg/mL in-reaction), which further diluted the 6-OHDA to a final concentration of 25 µM. Treated cells were incubated for 24 h. All subsequent assays, apart from the Ca^{2+} flux assay were assessed after 24 h exposure. The SRB assay was conducted as per Section 2.5 to evaluate protection against neurotoxin-induced cytotoxicity and used to normalise fluorescent data.

2.6.1. Effects on reactive oxygen species and reduced glutathione concentrations

The ROS and GSH concentrations were determined using the dihydrodichlorofluorescein diacetate (H_2-DCF-DA) cleavage and monochlorobimane (MCB) adduct formation assays (Kamencic *et al*., 2000), respectively. 2,2'-Azobis (2-methylpropionamide) dihydrochloride (AAPH; 1 mM in-reaction) and buthionine sulfoximine (1 mM in-reaction) was used as positive controls, respectively. After exposure to the crude extracts, 20 µL H_2-DCF-DA (220 µM prepared in PBS) or MCB (176 µM prepared in PBS) was added to cells and incubated for 2 h. Medium was replaced with 100 µL Hank's Balanced Salt Solution (HBSS), and the fluorescence measured with a H2 Synergy microplate reader (Biotek Inc, USA) at i) excitation = 485 nm and emission = 535 nm for ROS, and ii) excitation = 360 nm and emission = 460 nm for GSH. All values were blank-excluded, normalised to SRB absorbance data and intracellular ROS or GSH concentrations determined using the following equation:

$$\text{ROS or GSH concentration (\% of negative acidified control)} = \left(\frac{\text{RFIs}}{\text{RFIc}}\right) \times 100$$

where RFIs is the normalised, blank-excluded fluorescence of the sample, and RFIc is the average, normalised, blank-excluded fluorescence of the acidified negative control.

2.6.2. Effects on mitochondrial membrane potential

Mitochondrial membrane potential was monitored using the 5,5,'6,6'-tetrachloro-1,1,3,3'-tetraethylbenzimidazolylcarbocyanine iodide (JC-1) dye (Gravance *et al*., 2000). Tamoxifen (10 µM in reaction) was used as positive control. After exposure to the crude extracts, 20 µL JC-1 (150 µM prepared in PBS) was added and incubated for 30 min at 37˚C. Medium was replaced with 100 µL HBSS, and fluorescence measured at an excitation wavelength of 485 nm and an emission wavelength of 525 nm for the monomeric form of JC-1 dye, and at an excitation wavelength of 545 nm and the emission wavelength of 595 nm for the aggregate form of the JC-1 dye.

The JC-1 dye is a ratiometric dye, hence the ratio of the two emission wavelengths was used to normalise the data rather the SRB assay. All values were blank-excluded. The ratio and intracellular MMP was determined using the following equation:

$$\text{MMP (\% of negative acidified control)} = \left(\frac{\text{RFIs}}{\text{RFIc}}\right) \times 100$$

where RFIs is the normalised, blank-excluded fluorescence of the sample, and RFIc is the average, normalised, blank-excluded fluorescence of the acidified negative control.

2.7. Quantification of intracellular calcium flux

Intracellular Ca^{2+} was measured using the Ca^{2+} sensitive cationic dye, Fura-2 AM (Robinson *et al*., 2000). Ethylene glycol-bis(2-aminoethylether)-*N,N,N',N'*-tetraacetic acid (EGTA) (1 mM in-reaction) was used as positive control.

Cultured cells were washed twice with loading buffer (5.9 mM potassium chloride, 1.4 mM magnesium chloride, 10 mM 4-[2-hydroxyethyl]-1-piperazineethanesulfonic acid [HEPES], 1.2 mM monosodium phosphate, 5 mM sodium bicarbonate, 140 mM sodium chloride, 11.5 mM D-glucose and 1.8 mM calcium chloride). Cells were loaded with 10 µL of 1 mM Fura-2 AM and 5 µL of 20% Pluronic F127 to a final concentration 10 µM and 0.1%, respectively. Cells were incubated for 1 h at 37˚C, and subsequently centrifuged at 200 *g* for 5 min. The supernatant was discarded and cells were re-suspended in 6 mL HBSS. The cell suspension (60 µL) was added to white 96-well plates, and incubated for an additional 10 min at 37˚C. Subsequent to incubation, cells were read at the dual excitation wavelengths of 340 nm and 380 nm, and an emission wavelength of 508 nm every 1.53 min for 15 min to establish baseline readings. After an initial reading was obtained, 30 µL of 100 µM 6-OHDA was manually added to respective wells and read for 30 min. Crude extracts

(30 µL of 2, 4 , 20, 60 µg/mL in HBSS) were manually added and the fluorescence measured for a further 3 h. The final concentration of 6-OHDA was 25 µM and 0.5, 1, 5 and 15 µg/mL for crude extracts.

The Fura-2 AM dye is a ratiometric dye hence the ratio of the two emission wavelengths was used to normalise the data rather the SRB assay. All values were blank-excluded, ratio and intracellular calcium concentrations were determined using the following equation. A fluorescence ratio vs time curve, was used to calculate the area under the curve (AUC).

$$\text{Intracellular calcium (\% of acidified negative control)} = \left(\frac{\text{AUCs}}{\text{AUCc}}\right) \times 100$$

where AUCs is the normalised, blank-excluded area under the curve of the sample, and AUCc is the average, normalised, blank-excluded area under the curve of the acidified negative control.

2.7.1. Effects on intracellular adenosine triphosphate concentrations

The monitoring of ATP may be used as an adjunct to assist with determination of cell death (Lemasters *et al*., 1998). The ATP levels were determined using the ApoSENSOR ATP assay kit following the manufacturer's instructions. After 24 h exposure, culture medium was replaced with 90 µL ATP buffer (containing the ATP-monitoring enzyme). Luminescence was measured after 1 min of incubation using the H2 Synergy microplate reader and ATP concentrations determined using the following equation:

$$\text{ATP concentration (\% of acidified negative control)} = \left(\frac{\text{RLIs}}{\text{RLIc}}\right) \times 100$$

where RLIs is a blank-excluded luminescence of the sample, and RLIc is the average, blank-excluded luminescence of the acidified negative control.

2.7.2. Effects on cellular morphology

Cellular morphology was assessed using phase-contrast microscopy and polarisation-optical transmitted light differential interference contrast (PlasDIC) microscopy. Staurosporine (20 µM in-reaction) was used as an apoptotic control (Nkandeu *et al*., 2013). Cells were seeded and exposed in 24-well plates as described in Section 2.4 with appropriate adjustment to volumes. Microscopy images were taken using a Zeiss Axiovert-40 microscope (Göttingen, Germany) and Zeiss Axiovert MRm monochrome camera (Carl Zeiss MicroImaging GmbH, Göttingen, Germany). A magnification of 5x and 40x was used for phase contrast and PlasDIC microscopy, respectively. Two representative images per experiment were taken at the centre of each well.

2.8. Data analysis and statistics

All experiments were done with at least technical and biological triplicates (n≥9). Data was compiled using Microsoft Excel, and analysed using GraphPad Prism 5.0. Data was expressed as the mean ± standard error of

the mean (SEM). Non-linear regression was used to determine the IC_{50}. Statistical significance were assessed using the Kruskal Wallis test, using a post-hoc Dunn's test. Significance was taken as $p<0.05$.

3. Results and Discussion

3.1. Crude extract fingerprint and phytochemical profile

Using UPLC-HDMS, several phytochemicals were tentatively identified in the crude extracts (Table 1), and chemical profiles created (Figure 1). For *A. oppositifolia*, ouabagenin was detected in the acetone extract alone. Acetylnerbowdine, buphacetine and nerbowdine (detected in the methanol extract of *B. disticha*) were absent from the acetone extracts. No difference in the compounds extracted was observed for *X. undulatum*, however, this does not suggest the quantity of compounds are not different between the acetone and methanol extracts.

Apart from 3-, 4- and 5-caffeoylquinic acid, all others constituents have been described in *A. oppositifolia* previously (Hauschild-Rogat *et al*., 1967; Chen, 1970; Ezzat *et al*., 2016). The three former compounds thus appear to be a first-time description for *A. oppositifolia*. Acobioside A (Chen, 1970), acofrioside, acolongifloroside H and K, acovenoside C (Hauschild-Rogat *et al*., 1967), opposide (Chen, 1970), oppovenoside and ouabain (Hauschild-Rogat *et al*., 1967) have been identified in seeds, while acovenoside A has been detected from the epicarp of fruits previously (Ezzat *et al*., 2016).

The Amaryllidaceae-type alkaloids are well-described in *B. disticha*. Twelve major alkaloids have been detected in the bulbs: acetylnerbowdine, buphacetine, buphanamine (de Smet, 1996), buphanidrine (de Smet, 1996; Cheesman, 2013), buphanisine, crinamidine, crinine, distichamine (de Smet, 1996), 6α-hydroxycrinamine (Adewusi *et al*., 2012), lycorine, nerbowdine and undulatin (de Smet, 1996).

X. undulatum has been reported to contain all compounds identified in the present study (Kuritzkes *et al*., 1963; Ghorbani *et al*., 1997; Pauli and Fröhlich, 2000; Tschesche and Brathge, 2018; Tschesche *et al*., 2018). Apart from these, additional compounds have been described, including allouzarigenin, alloxysmalogenin, alloxysmalorin, ascleposide, coroglaucigenin-3-*O*-β-glucoside, desglucouzarin, desxgluoxysmalorin, pachygenol-3-*O*-β-glucoside, smalorin, uzaroside, xysmalogenin and xysmalorin (Kuritzkes *et al*., 1963; Ghorbani *et al*., 1997; Pauli and Fröhlich, 2000; Tschesche and Brathge, 2018; Tschesche *et al*., 2018).

3.2. Inherent cytotoxicity of crude extracts

For all three plants, acetone extracts were more cytotoxic than their respective methanol extracts. Given the similar polarity index of the solvents, the tentatively identified phytochemicals did not differ much between the extracts, however, the ratio thereof may influence the level of cytotoxicity seen due to combinational effects. Cytotoxicity data of these plants are scare, however, for those available, discrepancies could be due to different plant parts used, incubation time, extraction solvent, and varying cell lines tested against (Oleszek *et al*., 2002).

Table 1: Phytochemicals tentatively identified by UPLC-HMDS in the crude extracts of the plants investigated

Plant	Identified phytochemicals	Extract		Empirical formula	Monoisotopic molecular mass (Da)	Monoisotopic calculated mass (Da)	ESI mode	Fragments ions observed (Da)
		Acetone	Methanol					
A. oppositifolia	3-Caffeoylquinic acid	X	X	$C_{16}H_{18}O_9$	354.0951	353.0873	Negative	191.05; 179.03; 135.04
	4-Caffeoylquinic acid	X	X	$C_{16}H_{18}O_9$	354.0951	353.0873	Negative	191.05; 179.03; 173.04; 136.04
	5-Caffeoylquinic acid	X	X	$C_{16}H_{18}O_9$	354.0951	353.0873	Negative	191.05
	Acobioside A	X	X	$C_{36}H_{56}O_{14}$	712.3670	713.3748	Positive	551.3; 391.3; 373.2; 355.2
	Acobioside A isomer	X	X	$C_{36}H_{56}O_{14}$	712.3670	713.3748	Positive	551.3; 391.3; 373.2; 355.2
	Acolongifloroside K	X	X	$C_{29}H_{44}O_{12}$	584.2833	585.2911	Negative and positive	439.2; 403.2; 385.2; 373.2 (ESI+)
	Acovenoside A	X	X	$C_{30}H_{46}O_9$	550.3142	551.3220	Positive	391.2; 373.2; 355.2; 337.2
	Acovenoside B	X	X	$C_{32}H_{48}O_{10}$	592.3248	593.3326	Positive	433.2; 373.2; 355.2; 337.2
	Acovenosigenin (substructure)	X	X	$C_{23}H_{34}O_5$	390.2406	391.2485	Positive	373.23; 355.22; 337.21; 175.14
	Opposide	X	X	$C_{29}H_{44}O_{11}$	568.28836	569.2962	Negative and positive	433.1; 423.2; 339.2; 321.2 (ESI+)
	Ouabain	X	X	$C_{29}H_{44}O_{12}$	584.2833	585.2911	Negative and positive	439.2; 403.2; 385.2; 373.2 (ESI+)
	Ouabagenin (substructure)	X		$C_{23}H_{34}O_8$	438.2254	439.2332	Positive	403.2; 385.2; 373.2; 355.2
B. disticha	Acetylnerbowdine		X	$C_{19}H_{23}NO_6$	361.1525	362.1604	Positive	330.1294; 302.1360; 298.1051; 270.100
	Buphacetine analogue	X	X	$C_{20}H_{23}NO_7$	389.1475	390.1553	Positive	300.1219; 281.1041; 268.0931; 256.0938
	Buphacetine		X	$C_{20}H_{25}NO_7$	391.1631	392.1709	Positive	332.1542; 300.1272; 282.1105; 255.0836
	Buphanamine	X	X	$C_{17}H_{19}NO_4$	301.1314	302.1392	Positive	270.1091; 226.0830; 211.0718; 181.0627
	Buphanidrine	X	X	$C_{18}H_{21}NO_4$	315.1471	316.1549	Positive	284.1254; 269.1025; 254.1126; 226.0987
	Buphanisine	X	X	$C_{17}H_{19}NO_3$	285.1365	286.1443	Positive	254.1151; 239.0934; 226.0841; 196.0750
	Crinamidine	X	X	$C_{17}H_{19}NO_5$	317.1263	318.1341	Positive	286.1082; 268.0959; 227.0657; 191.0712
	Distichamine	X	X	$C_{18}H_{19}NO_5$	329.3470	330.1341	Positive	270.1091; 252.0991; 222.0882; 134.0599
	Epicrinine	X	X	$C_{16}H_{17}NO_3$	271.1208	272.1287	Positive	254.1161; 226.0849; 196.0749; 136.0754
	Lycorine	X	X	$C_{16}H_{17}NO_4$	287.1158	288.1236	Positive	270.1095; 252.1002; 226.0825; 181.0625
	Nerbowdine		X	$C_{17}H_{21}NO_5$	319.1420	320.1498	Positive	302.1360; 229.0852; 201.0889; 169.0650
	Undulatin	X	X	$C_{18}H_{21}NO_5$	331.1420	332.1498	Positive	282.1111; 271.0920; 243.0902; 211.0731
X. undulatum	Allouzarin	X	X	$C_{35}H_{54}O_{14}$	698.7949	697.3435	Negative and positive	535.28; 373.23; 291.17; 161.03
	Allouzarin	X	X	$C_{35}H_{54}O_{14}$	698.7949	699.3592	Positive	537.30; 375.25; 357.24; 339.23
	Coroglaucigenin	X	X	$C_{23}H_{34}O_5$	390.5200	391.2484	Positive	373.23; 355.22; 355.22; 337.21
	Frugoside	X	X	$C_{29}H_{44}O_9$	536.6620	537.3064	Positive	519.29; 375.24; 357.23; 339.23
	Pachygenol	X	X	$C_{23}H_{32}O_5$	388.4972	389.2328	Positive	371.22; 353.21; 335.20; 325.12
	Uzarigenin	X	X	$C_{23}H_{34}O_4$	374.5210	375.2535	Positive	357.25; 339.23; 325.11;
	Uzarin	X	X	$C_{35}H_{54}O_{14}$	698.8030	697.3435	Negative	535.29; 373.23; 161.04;
	Uzarin	X	X	$C_{35}H_{54}O_{14}$	698.8030	699.3592	Positive	537.30; 519.29; 375.24; 339.23

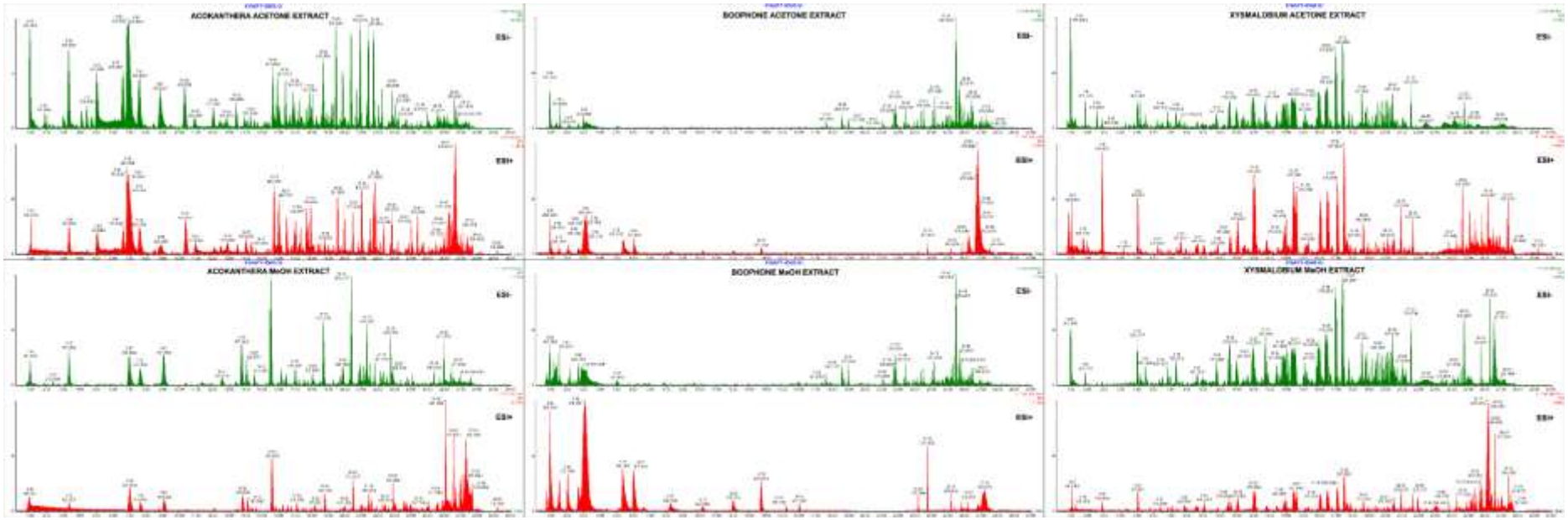

Figure 1: Chemical profiles of *A. oppositifolia*, *B. disthica* and *X. undulatum* crude extracts as determined by UPLC-HDMS.

The acetone and methanol crude extracts of *A. oppositifolia* had intermediate cytotoxicity with IC_{50} values of 30.5 µg/mL and 41.4 µg/mL, respectively. The literature support the cytotoxicity of *A. oppositifolia*. A dichloromethane extract of *A. oppositifolia* inhibited all cellular growth in the MCF-7 breast cancer cell line and UACC62 melanoma cell lines at 12.50 µg/mL and 6.25 µg/mL, respectively (Fouche *et al*., 2008). Furthermore, the cytotoxicity of the methanol crude extract of *A. oppositifolia* has been reported in human drug-sensitive CCRF-CEM leukaemia (IC_{50} = 2.5 µg/mL), multi-drug resistance CEM/ADR5000 leukaemia (IC_{50} = 2.83 µg/mL) (Saeed *et al*., 2016), and HepG2 hepatocarcinoma cell lines (IC_{50} = 26.63 µg/mL) (Cordier and Steenkamp, 2015). Ouabain has been shown to be toxic both *in vitro* (Pezzani *et al*., 2014) and *in vivo* (Lees *et al*., 1990), producing hippocampal necrosis in rat brains (Lees *et al*., 1990). Furthermore, acovenoside A, acolongifloriside K and opposide have been shown to be cytotoxic (Kingston and Reichstein, 1974).

The acetone extract of *B. disticha* was more cytotoxic (IC_{50} = 11.5 µg/ml) than its methanol counterpart (IC_{50} = 22.4 µg/mL). Adewusi *et al*. (2012) reported an IC_{50} of 27.3 µg/mL in SH-SY5Y cells for a methanol extract, proposing Amaryllidaceae alkaloids as the bioactive constituents. Of the compounds identified, cytotoxicity reports suggest that buphanamine (van Goietsenoven *et al*., 2010), buphanidrine (Nair *et al*., 2012) and buphanisine (van Goietsenoven *et al*., 2010) are not major contributing factors, while distichamine (Nair *et al*., 2012) and lycorine (van Goietsenoven *et al*., 2010; Nair *et al*., 2012) are more likely responsible for the activity noted. Lycorine was shown to induce cytotoxicity in glioma and astrocytoma cells at 6.9 and 7.6 µM, respectively (van Goietsenoven *et al*., 2010).*X. undulatum* was the most cytotoxic of all three plants studied, with IC_{50}'s of 2.8 µg/mL and 7.3 µg/mL for the acetone and methanol extract, respectively. *A. oppositifolia*, also a member of the Apocynaceae family, induced less cytotoxicity, indicating intra-family differences that could alter bioactivity (Joshi *et al*., 2004). The level of cytotoxicity observed in both extracts of *X. undulatum* is concerning due to the wide use of the herbal remedy. Cytotoxicity appears to be attributed to coroglaucigenin (Khorombi, 2016), frugoside (Kiuchi *et al*., 1998) and uzarin (Araya *et al*., 2012). Coroglaucigenin (Khorombi, 2016) and uzazrin (Kiuchi *et al*., 1998) have been reported as cytotoxic to a variety of cell lines. Frugoside displayed IC_{50} values between 0.03 µg/mL and 1.1 µg/mL (Kiuchi *et al*., 1998).

3.3. The effect of crude extracts on 6-hydroxydopamine-induced reduction in cell density

6-Hydroxydopamine, a validated neurotoxin for *in vitro* PD models (Lopes *et al*., 2010), is prone to auto-oxidation and precipitation. It was thus reconstituted in acidified medium supplemented with 0.1% ascorbic acid following suggestions proposed by the manufacturer (Lopes *et al*., 2010). No significant differences were observed between the negative control, vehicle control and acidified control for any parameters measured. All positive controls functioned as expected. 6-Hydroxydopamine reduced cell density by 91% (Figure 2).

Crude extracts of *A. oppositifolia, B. disticha,* and *X. undulutum* increased cell density between ~20 and ~50% after 24 h exposure (Figure 2). Lower concentrations of the crude extracts (<30 µg/mL) tended to offer greater cytoprotection than higher concentrations, suggesting additive cytotoxicity with 6-OHDA and limited beneficial use above a certain concentration. Due to this dose-dependent decrease in cytoprotection, subsequent

experiments explored lower concentrations of the crude extracts (0.5 to 15 µg/mL). Although both crude extracts of *X. undulatum* were the most cytotoxic of the three plants assayed, they displayed the greatest cytoprotection of all three plants after 6-OHDA-induced cytotoxicity.

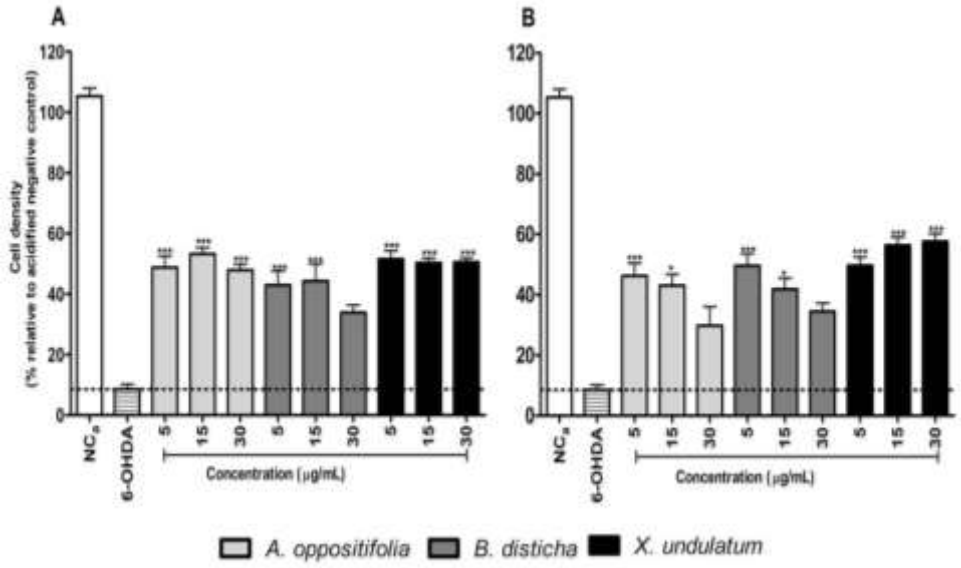

Figure 2: Cytoprotection offered by A) acetone and B) methanol crude extracts against 6-OHDA after 24 h exposure. 6-OHDA- 6-hydroxydopamine, NC_a- acidified negative control. Significant difference to the 6-OHDA treatment * $p < 0.05$, *** $p < 0.001$.

3.4. The effect of crude extracts on 6-hydroxydopamine-induced mitochondrial toxicity and oxidative stress

The 6-OHDA induced mitochondrial membrane depolarisation by 54.2% (Figure 3A, B) and ROS generation by 217.7%, (Figure 3C, D), however, unexpectedly increased GSH by 102.1% (Figure 3E, F). The literature supports the depolarisation observed, as 6-OHDA interferes with the ETC by blocking mitochondrial complex I with subsequent free radical production (Mazzio *et al*., 2004; Lopes *et al*., 2010; Esmaeili-Mahani *et al*., 2013). Twenty-four-hour exposure to 50 µM 6-OHDA has been reported to increase GSH levels, possibly due to adaptive *de novo* synthesis (Tirmenstein *et al*., 2005) to attenuate the ROS generation observed. Increased ROS concentrations stimulates the cellular antioxidant response element, which in turn promotes synthesis of endogenous antioxidants, like GSH, to combat oxidative stress (Pessayre *et al*., 2012).

None of the crude extracts significantly altered MMP (Figure 3A, B). The slight reduction noted for the acetone extract of *A. oppositifolia* may be attributed to ouabain, a known mitochondrial membrane depolariser (Chen *et al*., 2014). Since mitochondria are the most metabolically-active organelles, they are prone to injury. Ly *et al*. (2003) found that cytochrome c leaks out prior to mitochondrial membrane depolarisation, which will subsequently induce cytotoxicity (Ly *et al*., 2003), and is a common feature of apoptosis and necroptosis (Elmore,

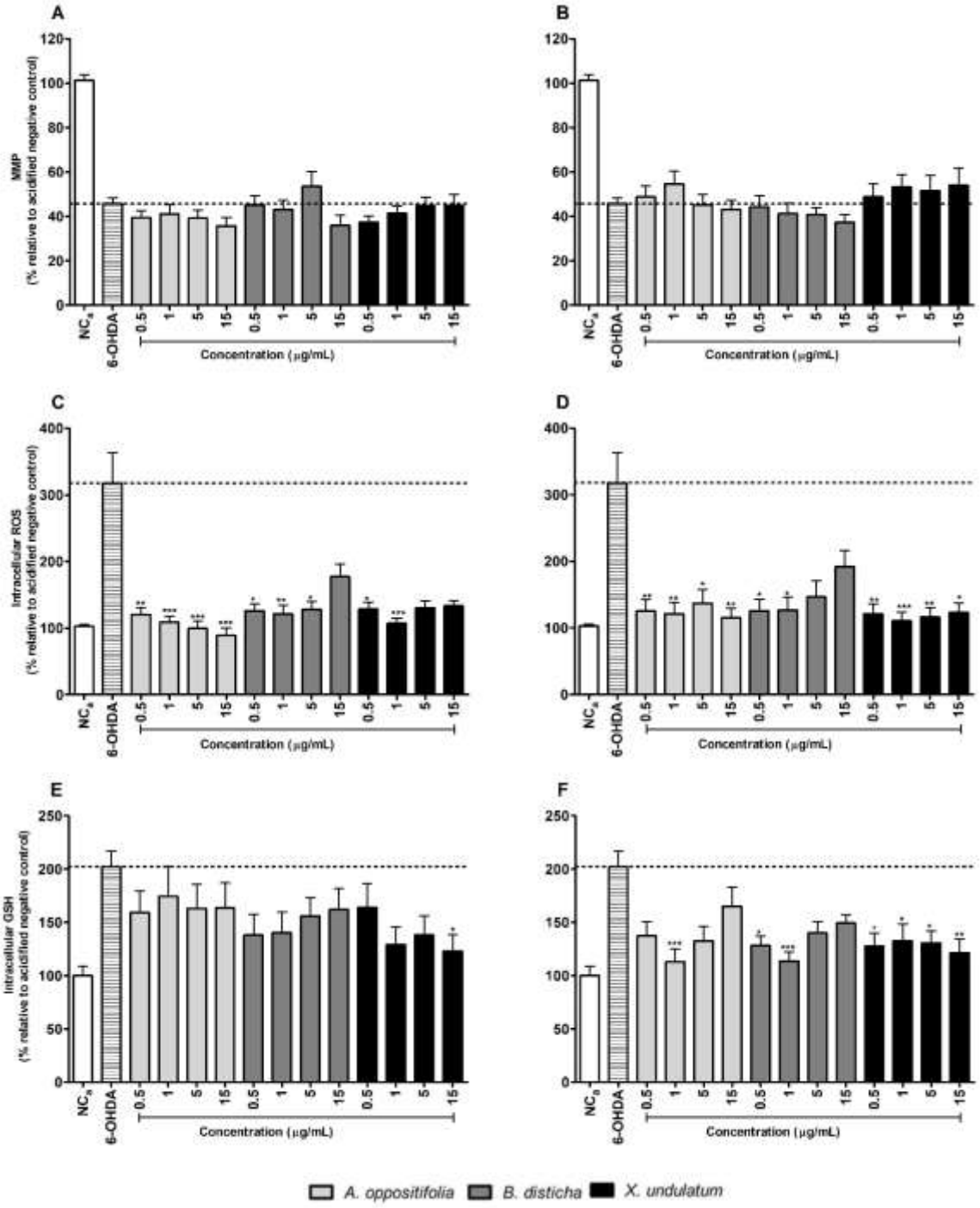

Figure 3: The effect of crude extracts on 6-OHDA-induced A and B) mitochondrial membrane depolarisation, C and D) ROS generation, and E and F) GSH increase after 24 h exposure. Figures A, C and E refer to acetone extracts, while B, D and F refer to methanol extracts. 6-OHDA- 6-hydroxydopamine, NC_a- acidified negative control. Acetone extracts on the left, methanol extracts on the right. Significant difference to the 6-OHDA treatment,* $p < 0.05$,** $p < 0.01$ and *** $p < 0.001$.

2007; Tait *et al*., 2014). As cytotoxicity was attenuated, but mitochondrial depolarisation unperturbed, extracts may only offer a protective effect downstream of mitochondrial toxicity. As such, underlying mitochondrial toxicity may persist and ultimately still induce cytotoxicity at a later time.

Although mitochondrial toxicity was not affected, both extracts of *A. oppositifolia* prevented 6-OHDA-induced oxidation by ~190% (Figure 3C, D). The literature supports the ability of these extracts to scavenge ROS (Sharma and Chaurasia, 2014). Both extracts of *B. disticha* displayed a greater activity at lower concentrations (~190% reduction), similar to that observed in the SRB assay (Figure 3C, D). Higher concentrations of *B. disticha* may thus aid in free radical production, hindering its ability to offer cytoprotection. It is unclear as to why antioxidant activity was present, as methanol extracts have been reported to lack activity in ABTS and DPPH assays (Adewusi *et al*., 2012). Both extracts of *X. undulatum* decreased 6-OHDA-induced ROS (Figure 2C, D) by ~190%, however, literature regarding its antioxidant activity could not be procured. As ROS may be created by auto-oxidation of 6-OHDA, it is possible that extracellular ROS may be depleted by the crude extracts rather than mitochondria-produced free radicals.

Although ROS was produced, 6-OHDA did not decrease GSH, but rather increased it. The methanol and acetone extract of *A. oppositifolia* prevented the GSH increase (Figure 3E, F) by ~30% to ~70%, however, was not dose-dependent. This preventative effect could suggest a homeostatic control to reverse any alterations that 6-OHDA may cause when compared to an untreated environment, or potentially conjugation to GSH as a by-product of detoxification. Both extracts of *B. disticha* and *X. undulatum* (Figure 3E, F) displayed a trend to reduce the 6-OHDA-induced increase in GSH. The mechanism of ROS neutralisation used by the crude extracts does not appear to involve intracellular GSH, and thus requires further investigation. No literature could be found to highlight specific compounds in the cytoprotection observed for the ROS and GSH assays.

3.5. The effect of crude extracts on 6-OHDA-induced decreased intracellular adenosine tri-phosphate

Treatment with 6-OHDA decreased ATP by 66.5% (Figure 4). The acetone and methanol extracts of *A. oppositifolia* and *B. disticha*, respectively, dose-dependently increased ATP levels at <15 µg/mL by ~35%. However, at 15 µg/mL, the effect on ATP was not as prominent (Figure 4). This effect supports the greater cytoprotection offered by lower concentrations, and the potential for additive cytotoxicity at higher concentrations. The methanol extracts of *A. oppositifolia* and *X. undulatum* displayed a plateaued effect, maintaining ATP levels at ~60% of normal (Figure 4). Although the crude extracts did not attenuate the decreased MMP, they did improve ATP levels, suggesting that the crude extract may potentiate the glycolytic pathway rather than oxidative phosphorylation. The extracts could still be beneficial in PD, as one of the triggers for neuronal cell death is ATP depletion (Ly *et al*., 2003; Bhat *et al*., 2015). Several of the compounds identified in *A. oppositifolia* (acovenoside A [Hafner *et al*., 2017] and ouabain [Erdmann and Schoner, 1974]), *B. disthica* (lycorine [Chen *et al*., 2015]) and *X. undulatum* (uzarin [Abbott *et al*., 1998]) are ATPase inhibitors. In such a way, the aforementioned phytochemicals may prevent ATP-hydrolysis from occurring, thus allowing for increased ATP levels.

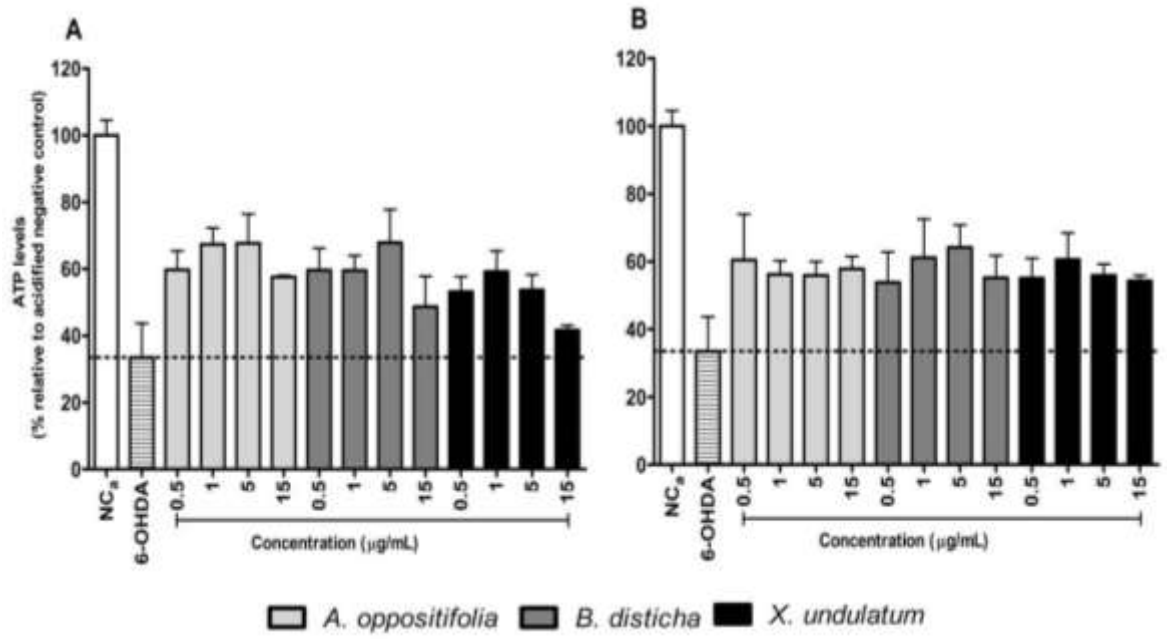

Figure 4: Increase of ATP after 24 h treatment with A) acetone and B) methanol crude extracts in the 6-OHDA neurotoxicity model. 6-OHDA- 6-hydroxydopamine, NC_a- acidified negative control.

3.7. The effect of crude extracts and 6-OHDA-induced alterations on intracellular calcium flux

The exposure of cells to 6-OHDA decreased intracellular Ca^{2+} levels by 17% (Figure 5). Extracts of *A. oppositifolia* displayed a dose-dependent decrease (16 – 38% for acetone, and 23-48% for methanol) in intracellular Ca^{2+} levels relative to the negative control (Figure 5). The extracts of *B. disticha* maintained constant levels (~80% of normal) of intracellular Ca^{2+} across the concentrations tested (Figure 5). The acetone extract of *X. undulatum* displayed a dose-dependent decrease (17 - 25%) in intracellular Ca^{2+} levels. None of the crude extracts normalised intracellular Ca^{2+} levels to basal levels. Even more so, the extracts of *A. oppositifolia* potentiated a further decrease in intracellular Ca^{2+} levels. Ouabain (identified in *A. oppositifolia*) has been reported to both increase intracellular Ca^{2+} levels (Xu *et al*., 2010) or prevent accumulation thereof; the latter is due inhibition of the mitochondrial sodium-calcium exchanger (O'Rourke and Liu, 2012). The latter may account for the effects observed.

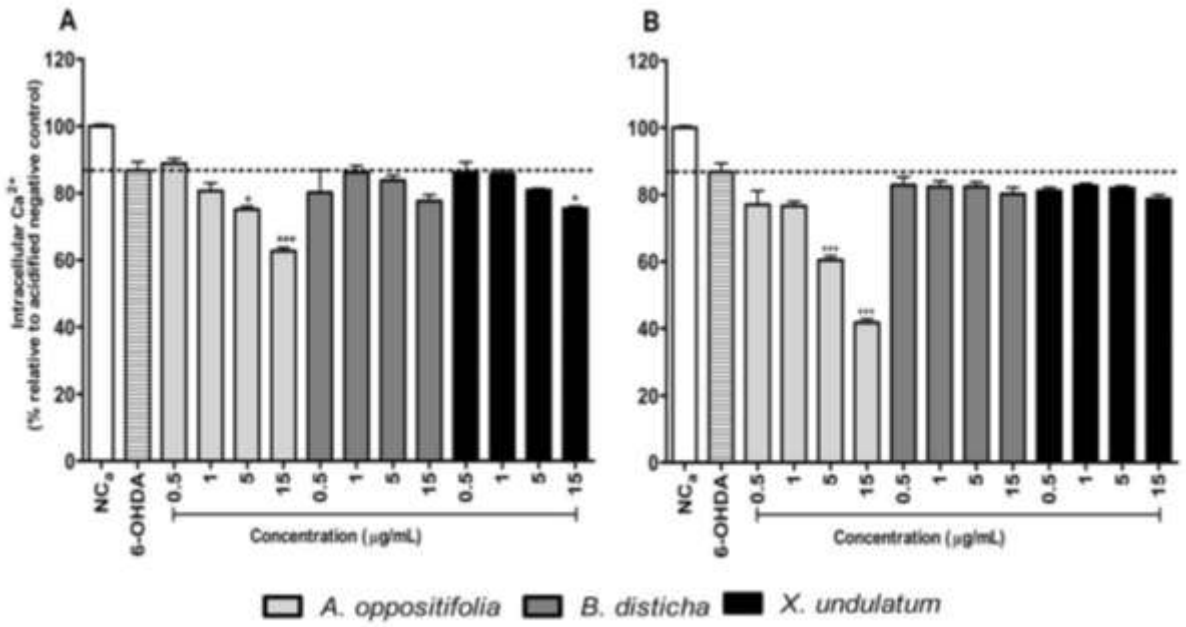

Figure 5: Additional Ca^{2+} reducing effect of A) acetone and B) methanol crude extracts on 6-OHDA-induced calcium decrease after 24 h exposure. 6-OHDA- 6-hydroxydopamine, NC_a- acidified negative control. Significant difference to the 6-OHDA treatment,* $p < 0.05$,** $p < 0.01$ and *** $p < 0.001$.

3.8. The effect of plant extracts and 6-OHDA on cellular morphology

Micrographs show that 6-OHDA reduced cell density and increased the roundedness of cells (Figure 6), a feature consistent with apoptosis (Elmore, 2007). Cell density and morphological integrity was greater when exposed to acetone extracts of *A. oppositifolia*, suggesting higher cytoproprotection than with methanol extracts (Figure 6). The latter is consistent with the results obtained from the SRB assay (Figure 2). A low concentration (0.5 µg/mL) of both extracts *of B. disticha* displayed better cytoprotective effects than the 5 µg/mL treated cells (Figure 6); the same trend was observed in the cytotoxicity assay (Figure 2). Both extracts of *X. undulatum* showed comparable cytoprotection which was not dose-dependent (Figure 6). Even though the mode of cell death was not deduced, crude extracts were still able to improve cell viability, thus creating a platform for further studies.

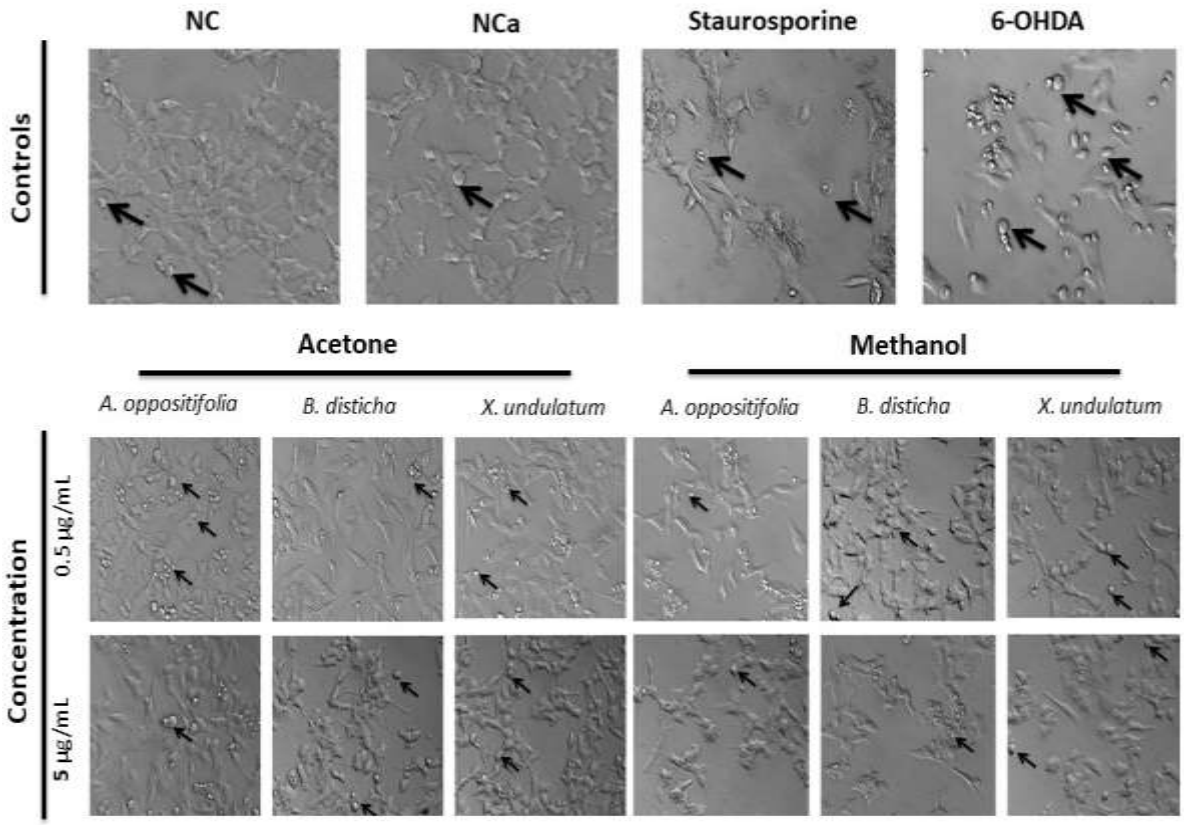

Figure 6: The effect of extracts and 6-OHDA on cellular morphology of the SH-SY5Y cell line using PlasDIC. NC (negative control), NC_a (acidified negative control) and staurosporine (20 µM) served as controls. A magnification of 40x was used, and arrows indicate apoptotic bodies. 6-OHDA- 6-hydoxydopamine

4. Conclusion

The neurotoxin, 6-OHDA, induced PD-like effects in the SH-SY5Y cell line, creating a model to study PD *in vitro*. Various phytochemicals were tentatively identified in the crude extract of *A. oppositifolia, B. disticha* and *X. undulatum*. The crude extracts showed cytoprotective effects against 6-OHDA-induced cytotoxicity. This appeared to be linked to reduced ROS generation, but not mitochondrial protection or Ca^{2+} regulation. Adenosine tri-phosphate levels were maintained, suggesting unperturbed bioenergetics. Morphology studies supported the cytoprotective effects induced by the crude extracts. Of note is that lower concentrations of the crude extracts (0.5 -5 µg/mL) offered greater cytoprotective activity, suggesting a potent effect that warrants further isolation studies. Although cell density and ATP levels were increased by the crude extracts, it does appear that mitochondrial toxicity was unaffected, suggesting that phytochemicals are not deterring mitochondrial toxicity. This may result in delayed cytotoxicity.

Although the greatest level of cytoprotection was offered by *X. undulatum*, it is important to mention that the extracts themselves were highly cytotoxic, which may bolster further development. Additionally, it is widely accepted that by the time PD symptoms are evident, more than 80% of the neurons have been lost and the

remaining neurons will also die despite dopamine replacement therapy (Dauer and Przedborski, 2003; Ren *et al*., 2015). However, in this study crude extracts of *A. oppositifolia, B. disticha* and *X. undulatum* were able to maintain consistent cell density providing cytoprotection. This indicates that the plants alone will not cure PD but they may potentially be used as adjuncts to current PD treatment to preserve existing dopaminergic neurons. Future studies are required to elucidate the mode of cell death used by 6-OHDA as well as the potential mitochondrial targets that sustains ATP production to stimulate survival.

5. Acknowledgements

The authors would like to acknowledge the University of Pretoria RESCOM-SOM for funding.

6. References

Abeti, R., Abramov, A.Y., 2015. Mitochondrial Ca^{2+} in neurodegenerative disorders. Pharmacological Research 99, 377-381.

Abbott, A., Holoubek, C., Martin, R., 1998. Inhibition of Na+,K+-ATPase by the cardenolide 6'-O-(E-4-hydroxycinnamoyl) desglucouzarin. Biochemical and Biophysical Research Communications 251, 256-259.

Adedapo, A.A., Jimoh, F.O., Afolayan, A.J., Masika, P.J., 2008. Antioxidant activities and phenolic contents of the methanol extracts of the stems of *Acokanthera oppositifolia* and *Adenia gummifera*. BMC Complementary and Alternative Medicine 8, 54-61.

Adewusi, E., Fouche, G., Steenkamp, V., 2012. Cytotoxicity and acetylcholinesterase inhibitory activity of an isolated crinine alkaloid from *Boophane disticha* (Amaryllidaceae). Journal of Ethnopharmacology 143, 572-578.

Adewusi, E.A., Fouche, G., Steenkamp, V., 2012. Antioxidant, acetylcholinesterase inhibitory activity and cytotoxicity assessment of the crude extracts of *Boophane disticha*. African Journal of Pharmacology and Therapeutics 1, 78-83.

Araya, J.J., Kindscher, K., Timmermann, B.N., 2012. Cytotoxic cardiac glycosides and other compounds from *Asclepias syriaca*. Journal of Natural Products 75, 400-407.

Banerjee, R., Starkov, A.A., Beal, M.F., Thomas, B., 2009. Mitochondrial dysfunction in the limelight of Parkinson's disease pathogenesis. Biochimica et Biophysica Acta 1792, 651-663.

Bharath, S., Hsu, M., Kaur, D., Rajagopalan, S., Andersen, J.K., 2002. Glutathione, iron and Parkinson's disease. Biochemical Pharmacology 64, 1037-1048.

Bhat, A.H., Dar, K.B., Anees, S., Zargar, M.A., Masood, A., Sofi, M.A., Ganie, S.A., 2015. Oxidative stress, mitochondrial dysfunction and neurodegenerative diseases; a mechanistic insight. Biomedicine & Pharmacotherapy 74, 101-110.

Blum, D., Torch, S., Lambeng, N., Nissou, M.-F., Benabid, A.-L., Sadoul, R., Verna, J.M., 2001. Molecular pathways involved in the neurotoxicity of 6-OHDA, dopamine and MPTP: contribution to the apoptotic theory in Parkinson's disease. Progress in Neurobiology 65, 135-172.

Cabezas, R., Avila, M.F., Torrente, D., El-Bachá, R.S., Morales, L., Gonzalez, J., Barreto, G.E., 2013. Astrocytes role in Parkinson: A double-edged sword. Neurodegenerative Diseases 10, 491-517.

Cairns, R.A., Harris, I.S., Mak, T.W., 2011. Regulation of cancer cell metabolism. Nature Reviews Cancer 11, 85-95.

Chen, D., Song, M., Mohamad, O., Yu, S., 2014. Inhibition of Na^+/K^+-ATPase induces hybrid cell death and enhanced sensitivity to chemotherapy in human glioblastoma cells. BMC Cancer 14, 716.

Chen, K.K., 1970. Newer cardiac glycosides and aglycones. Journal of Medical Chemistry 13, 1029-1034.

Chen, S., Jin, G., Huang, K.-M., Ma, J.-J., Wang, Q., Ma, Y., Tang, X.-Z., Zhou, Z.-J., Hu, Z.-J., Wang, J.-Y., Qin, A., Fan, S.-W., 2015. Lycorine suppresses RANKL-induced osteoclastogenesis *in vitro* and prevents ovariectomy-induced osteoporosis and titanium particle-induced osteolysis *in vivo*. Scientific Reports 5, 12853.

Contreras, L., Drago, I., Zampese, E., Pozzan, T., 2010. Mitochondria: The calcium connection. Biochimica et Biophysica Acta 1797, 607-618.

Cordier, W., Steenkamp, V., 2015. Evaluation of four assays to determine cytotoxicity of selected crude medicinal plant extracts *in vitro*. Britsh Journal of Pharmaceutical Research 7, 16-21.

Dauer, W., Przedborski, S., 2003. Parkinson's disease: Mechanisms and models. Neuron 39, 889-909.

de Smet, P., 1996. Some ethnopharmacological notes on African hallucinogens. Journal of Ethnopharmacology 50, 141-146.

Elmore, S., 2007. Apoptosis: a review of programmed cell death. Toxicologic Pathology 35, 495-516.

Erdmann, E., Schoner, W., 1974. Ouabain-receptor interactions in (Na^++K^+)-ATPase preparations. Naunyn-Schmiedebergs Archives of Pharmacology 83, 335-356.

Esmaeili-Mahani, S., Vazifekhah, S., Pasban-Aliabadi, H., Abbasnejad, M., Sheibani, V., 2013. Protective effect of orexin-A on 6-hydroxydopamine-induced neurotoxicity in SH-SY5Y human dopaminergic neuroblastoma cells. Neurochemistry International 63, 719-725.

Ezzat, S.M., El Gaafary, M., El Sayed, A.M., Sabry, O.M., Ali, Z.Y., Hafner, S., Schmiech, M., Jin, L., Syrovets, T., Simmet, T., 2016. The cardenolide glycoside acovenoside A affords protective activity in doxorubicin-induced cardiotoxicity in mice. Journal of Pharmacology and Experimental Therapeutics 358, 262-270.

Fouche, G., Cragg, G.M., Pillay, P., Kolesnikova, N., Maharaj, V.J., Senabe, J., 2008. *In vitro* anticancer screening of South African plants. Journal of Ethnopharmacology 119, 455-461.

Ghorbani, M., Kaloga, M., Frey, H.-H., Mayer, G., Eich, E., 1997. Phytochemical reinvestigation of *Xysmalobium undulatum r*oots (Uzara). Planta Medica 63, 343-346.

Gravance, C.G., Garner, D.L., Baumber, J., Ball, B.A., 2000. Assessment of equine sperm mitochondrial function using JC-1. Theriogenology 53:1691-1703.

Hafner, S., El Gaafary, M., Schmiech, M., Syrovets, T., Simmet, T., 2017. The cardenolide glycoside acovenoside A impedes proliferation of lung adenocarcinoma cells *in vitro* and *in vivo*. Federation of American Societies for Experimental Biology Journal 31, 996.10.

Ham, A., Lee, S.-J., Shin, J., Kim, K.-H., Mar, W., 2012. Regulatory effects of costunolide on dopamine metabolism-associated genes inhibit dopamine-induced apoptosis in human dopaminergic SH-SY5Y cells. Neuroscience Letters 507, 101-105.

Hauschild-Rogat, P., Weiss, E., Reichstein, T., 1967. Die cardenolide von *Acokanthera oppositifolia* (Lam.) CODD. 3. Mitteilung. Isolierung weitere Cardenolide und teilweise Strukturaufklärung. Glykoside und Aglykone, 301. Mitt. Helvetica Chimica Acta 50, 2299-2321.

Joshi, K., Chavan, P., Warude, D., Patwardhan, B., 2004. Molecular markers in herbal drug technology. Current Science 87, 159-165.

Kakkar, A.K., Dahiya, N., 2015. Management of Parkinson's disease: Current and future pharmacotherapy. European Journal of Pharmacology 750, 74-81.

Kamencic, H., Lyon, A., Paterson, P.G., Juurlink, B.H., 2000. Monochlorobimane fluorometric method to measure tissue glutathione. Analytical Biochemistry 286, 35-37.

Khorombi, T., 2016. A chemical and pharmacological investigation of three South African plants. University of KwaZulu-Natal, Dissertation.

Kim, S.W., Ko, H.S., Dawson, V.L., Dawson, T.M., 2006. Recent advances in our understanding of Parkinson's disease. Drug Discovery Today: Disease Mechanisms 2, 427-433.

Kingston, D., Reichstein, T., 1974. Cytotoxic cardenolides from *Acokanthera longiflora* Stapf. and related species. Journal of Pharmaceutical Sciences 63, 462-464.

Kiuchi, F., Fukao, Y., Maruyama, T., Obata, T., Tanaka, M., Sasaki, T., Mikage, M., Haque, M.E., Tsuda, Y., 1998. Cytotoxic principles of a Bangladeshi crude drug, akond mul (roots of *Calotropis gigantea* L.). Chemical and Pharmaceutical Bulletin 46, 528-530.

Kuritzkes, A.M., Tamm, C., Jäger, H., Reichstein, T., 1963. Die glykoside von *Xysmalobium undulatum* R. Br. dritte mitteilung. Glykoside und aglykone, 242. Mitteilung. Helvetica Chimica Acta 46, 8-23.

Lees, A.J., Hardy, J., Revesz, T., 2009. Parkinson's disease. Lancet 373, 2055-2066.

Lees, G., Lehmann, A., Sandberg, M., Hamberger, A., 1990. The neurotoxicity of ouabain, a sodium-potassium ATPase inhibitor, in the rat hippocampus. Neuroscience Letters 120, 159-162.

Lemasters, J.J., Nieminen, A.-L., Qian, T., Trost, L.C., Elmore, S.P., Nishimura, Y., Crowe, R.A., Cascio, W.E., Bradham, C.A., Brenner, D.A., Herman, B., 1998. The mitochondrial permeability transition in

cell death: a common mechanism in necrosis, apoptosis and autophagy. Biochimica et Biophysica Acta 136, :177-196.

Lopes, F.M., Schröder, R., da Frota Júnior, M.L.C., Zanotto-Filho, A., Müller, C.B., Pires, A.S., Meurer R.T., Colpo, G.D., Gelain, D.P., Kapczinski, F., Moreira, J.C., 2010. Comparison between proliferative and neuron-like SH-SY5Y cells as an *in vitro* model for Parkinson disease studies. Brain Research 1337, 85-94.

Ly, J.D., Grubb, D., Lawen, A., 2003. The mitochondrial membrane potential (Δψm) in apoptosis; an update. Apoptosis 8, 115-128.

Mazzio, E.A., Reams, R.R., Soliman, K.F., 2004. The role of oxidative stress, impaired glycolysis and mitochondrial respiratory redox failure in the cytotoxic effects of 6-hydroxydopamine *in vitro*. Brain Research 1004, 29-44.

McBean, G.J., Aslan, M., Griffiths, H.R., Torrão, R.C., 2015. Thiol redox homeostasis in neurodegenerative disease. Redox Biology 5, 186-194.

Nair, J.J., Rárová, L., Strnad, M., Bastida, J., van Staden, J., 2012. Apoptosis-inducing effects of distichamine and narciprimine, rare alkaloids of the plant family Amaryllidaceae. Bioorganic & Medicinal Chemistry Letters 22, 6195-6199.

Nair, J.J., van Staden, J., 2014. Traditional usage, phytochemistry and pharmacology of the South African medicinal plant *Boophone disticha* (L.f.) Herb. (Amaryllidaceae). Journal of Ethnopharmacology 151, 12-26.

Nkandeu, D.S., Mqoco, T.V., Visagie, M.H., Stander, B.A., Wolmarans, E., Cronje, M.J., Joubert, A.M., 2013. *In vitro* changes in mitochondrial potential, aggresome formation and caspase activity by a novel 17-β-estradiol analogue in breast adenocarcinoma cells. Cell Biochemistry and Function 31, 566-574.

O'Rourke, B., Liu, T., 2012. Methods for treating heart failure by inhibiting the mitochondrial sodium-calcium exchanger (MNCE). Patent US 2012/0077763 A1.

Oleszek, W., Stochmal, A., Karolewski, P., Simonet, A.M., Macias, F.A., Tava, A., 2002. Flavonoids from *Pinus sylvestri*s needles and their variation in trees of different origin grown for nearly a century at the same area. Biochemical Systematics and Ecology 30, 1011-1022.

Pauli, G.F., Fröhlich, R., 2000. Chiral key positions in Uzara steroids. Phytochemical Analysis 11, 79-89.

Pessayre, D., Fromenty, B., Berson, A., Robin, M-A., Lettéron, P., Moreau, R., Mansouri, A., 2012. Central role of mitochondria in drug-induced liver injury. Drug Metabolism Reviews 44, 34-87.

Pezzani, R., Rubin, B., Redaelli, M., Radu, C., Barollo, S., Cicala, M.V., Salvà, M., Mian, C., Mucignat-Caretta, C., Simioni, P., Iacobone, M., Mantero, F., 2014. The antiproliferative effects of ouabain and everolimus on adrenocortical tumor cells. Endocrine Journal 61, 41-53.

Reddy, P.H., Reddy, T.P., 2011. Mitochondria as a therapeutic target for aging and neurodegenerative diseases. Current Alzheimer Research 8, 393-409.

Ren, R., Sun, Y., Zhao, X., Pu, X., 2015. Recent advances in biomarkers for Parkinson's disease focusing on biochemicals, omics and neuroimaging. Clinical Chemistry and Laboratory Medicine 53, 1495-1506.

Robinson, J.A., Jenkins, N.S., Holman, N.A., Roberts-Thomson, S.J., Monteith, G.R., 2000. Ratiometric and nonratiometric Ca^{2+} indicators for the assessment of intracellular free Ca^{2+} in a breast cancer cell line using a fluorescence microplate reader. Journal of Biochemistry and Biophysical Methods 58, 227-237.

Ruszkiewicz, J., Albrecht, J., 2015. Changes in the mitochondrial antioxidant systems in neurodegenerative diseases and acute brain disorders. Neurochemistry International 88, 66-72.

Saeed, M.E., Meyer, M., Hussein, A., Efferth, T., 2016. Cytotoxicity of South-African medicinal plants towards sensitive and multidrug-resistant cancer cells. Journal of Ethnopharmacology 186, 209-223.

Sharma, P., Chaurasia, S., 2014. Evaluation of total phenolic, flavonoid contents and antioxidant activity of *Acokanthera oppositifolia* and *Leucaena leucocephala*. International Journal of Pharmacognosy and Phytochemical Research 7, 175-180.

Stafford, G.I., Pedersen, M.E., van Staden, J., Jäger, A.K., 2008. Review on plants with CNS-effects used in traditional South African medicine against mental diseases. Journal of Ethnopharmacology 119, 513-537.

Stayte, S., Vissel, B., 2014. Advances in non-dopaminergic treatments for Parkinson's disease. Frontiers in Neuroscience 8, 113-139.

Tait, S.W., Ichim, G., Green, D.R., 2014. Die another way–non-apoptotic mechanisms of cell death. Journal of Cell Science 127, 2135-2144.

Tirmenstein, M.A., Hu, C.X., Scicchitano, M.S., Narayanan, P.K., McFarland, D.C., Thomas, H.C., Schwartz, L.W., 2005. Effects of 6-hydroxydopamine on mitochondrial function and glutathione status in SH-SY5Y human neuroblastoma cells. Toxicology In Vitro 19, 471-479.

Tschesche, R., Brathge, K.-H., 2018. Über pflanzliche Herzgifte, XIX. Mitteil.: Die glykoside der Uzara-Wurzel. Chemische Berichte 85, 1042-1056.

Tschesche, R., Freytag, W., Snatzke, G., 2018. Über pflanzliche Herzgifte, XXXIX. Die konstitution des Xysmalogenins und über das vorkommen von allo-uzarigenin in Uzara-Wurzeln. Chemische Berichte 92, 3053-3063.

van Goietsenoven, G., Andolfi, A., Lallemand, B., Cimmino, A., Lamoral-Theys, D., Gras, T., Abou-Donia, A., Dubois, J., Lefranc, F., Mathieu, V., Kornienko, A., Kiss, R., Evidente, A., 2010. Amaryllidaceae alkaloids belonging to different structural subgroups display activity against apoptosis-resistant cancer cells. Journal of Natural Products 73, 1223-1227.

van Wyk, B.E., van Oudtshoorn B., Gericke, N., 2009. Medicinal Plants of South Africa. Briza.

Vichai, V., Kirtikara, K., 2006. Sulforhodamine B colorimetric assay for cytotoxicity screening. Nature Protocols 1, 1112-1116.

Xu, Z.-W., Wang, F.-M., Gao, M.-J., Chen, X.-Y., Hu, W.-L., Xu, R.-C., 2010. Targeting the Na^+/K^+-ATPase alpha1 subunit of hepatoma HepG2 cell line to induce apoptosis and cell cycle arresting. Biological and Pharmaceutical Bulletin 33, 743-751.

Yadav, H.P., Li, Y., 2015. The development of treatment for Parkinson's disease. Advances in Parkinson's Disease 4, 59-78.

.